Bull. Chem. Soc. Jpn., **53**, 3054—3058 (1980) [Vol. 53, No. 11

The Raman Spectra of Aligned Thin Films of Nematic Liquid Crystals

Haruka Yamada,* Keiji Fukumura, and Bun-ichi Tamamushi†
Department of Chemistry, Kwansei Gakuin University, Nishinomiya, Hyogo 662
† *Nezu Chemical Institute, Musashi University, Tokyo 176*

(Received November 27, 1979)

The Raman spectra of thin films of nematic liquid crystals, MBBA and NP-5A, have been measured for samples sandwiched between two glass (or quartz) plates, which had been pretreated in several ways. The intensities of the fundamental bands of the molecules and the polarization components of each band depend on the molecular orientation structures, such as the homogeneous and homeotropic alignments. The intensity ratio provides a semi-quantitative measure for the molecular orientation, and the Raman results are compared with those from polarizing microscopic observations and infrared spectra. The molecular orientation of the liquid crystals varies with the concentrations of surface-active agents as well as the materials used for the pretreatment of the plates. The molecular interactions, which give rise to the orientation structures, are briefly discussed.

The molecular orientation structures in nematic liquid crystals depend on the nature of the substrate surfaces resulting from previous treatment, and they can usually be distinguished by observation with a polarizing microscope.[1,2] They have, however, not always been clarified in molecular dimensions, because X-ray studies are not so effective for the thin films. Recently, the Raman spectra of liquid crystals have been actively studied,[3–7] but most of the work has been performed with bulk samples. For the vibrational spectra of liquid crystal films, we have reported a preliminary Raman result,[8] while some works on the far-infrared spectra have been reported[9–11] and the infrared ATR spectra on the In_2O_3 surface have been studied.[12] However, with the samples between glass or quartz plates, infrared measurement is not so useful. In order to obtain more precise information regarding the molecular orientation structures, the Raman spectra of thin films of nematic liquid crystals on glass or quartz surfaces have been studied in our present work.

Experimental

MBBA(*N*-(*p*-methoxybenzylidene)-*p*-butylaniline; Kodak and Tokyo Chem. Co.) and NP-5A (a mixture of 4-methoxy-4′-butylazoxybenzene with 4-methoxy-4′-ethylazoxybenzene; Merck) were used. Optically flat glass (or quartz) plates (25×75×1 mm) were cleaned by using a chromium trioxide solution and then treated by one of the following ways: (i) Silk treatment (rubbed with a silk cloth in the direction parallel to the long edges of the plate surface); (ii) HTAB treatment (dipped in an aqueous solution (0.007—1.4 mM; 1 M=1 mol dm^{-3}) of HTAB (hexadecyltrimethylammonium bromide; Wako Chem.) and then carefully dried); (iii) Lecithin treatment (dipped in an ethanol solution (0.001—1.0 mM) of lecithin (Wako 1st grade, extracted from eggs) and dried), or (iv) Silane treatment (dipped in a solution of 2 mM diphenyldichlorosilane (Wako Chem. special grade) in toluene and dried). A drop of MBBA or NP-5A was sandwiched by two pretreated plates, slightly pressed, and then fastened with a plastic tape along the edges. The thicknesses of the films were measured roughly by observing the interference fringes in the visible and infrared regions, 1—100 μm.

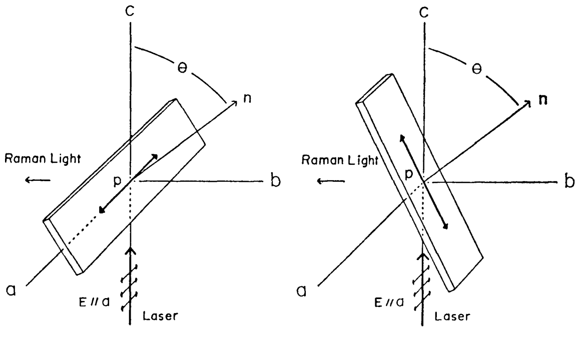

(A) p//E (B) p⊥E

Fig. 1. Setting and irradiation of samples: (A) ***p***//***E***, (B) ***p***⊥***E***.

For polarizing microscopic observation, the samples were examined between crossed nicols under a Carl Zeiss photomicroscope (64 fold).

The Raman spectra were measured by means of a JASCO R-300 spectrophotometer with a JEOL-04 Ar ion laser. All the observations of the films were made in oblique settings, where the plane normal of the film, n, made an angle, θ, with the incident beam (θ=30°—80°). The laser beam irradiated the sample along the c axis (a, b, and c are the space fixed Cartesian coordinates, and n lies on the bc plane), and the scattered light was gathered in the b direction, as is shown in Fig. 1.

For the measurements of the polarization components of the Raman bands, a usual polarizer was inserted in front of the sample and an analyzer was placed near the entrance slit of the monochromator. The electric vector of the laser beam, ***E***, was taken as the a direction and could be rotated in the b direction by means of a $\lambda/2$ plate made of white mica.

The infrared spectra were measured with a JASCO DS-402G infrared spectrophotometer for the samples on quartz plates. The polarized spectra were measured with an AgCl polarizer which was located in front of the thermocouple detector.

Results and Discussion

Examination in a polarizing microscope showed different patterns for the samples, as is shown in Table 1. For example, the sample of MBBA on the glass treated with silk showed a characteristic thready texture parallel to the long edges, ***p***, and is called as a homogeneous sample, while the sample of MBBA on the glass treated with the 0.7 mM HTAB solution showed only dark stars and is designated as a homeotropic sample. In Table 1 the samples which showed colorful patterns (including texture) are classified as //, and the samples with dark stars, as ⊥. There can be seen

Table 1. Results of observations by means of a polarizing microscope

Surface treatment		MBBA	NP-5A
HTAB (aq soln)	0.0070 mM	△	⊥
	0.070	⊥	⊥
	0.70	⊥	‖
	1.4	⊥	‖
Lecithin (C_2H_5OH soln)	0.0010 mM	‖	⊥
	0.010	‖	⊥
	0.10	⊥	⊥
	1.0	⊥	‖
Silane		‖	‖
Silk		‖ (texture)	‖ (texture)

⊥: Dark stars, ‖ : colorful pattern, △: dark colorful pattern.

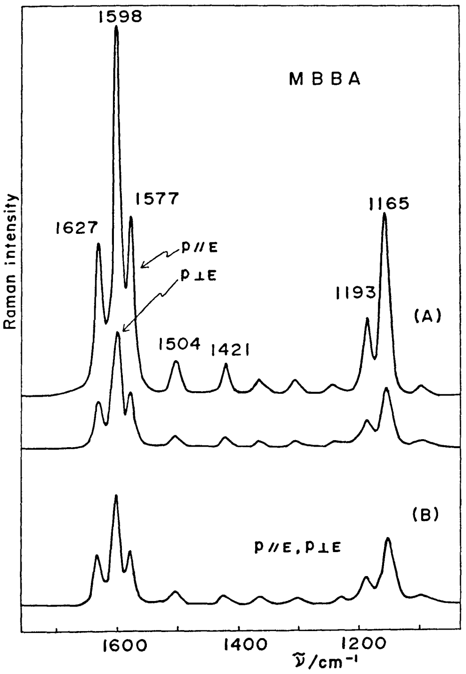

Fig. 2. Raman spectra of aligned thin (*ca.* 1 μm) films of MBBA.
(A): Homogeneous, (B) homeotropic samples.

only a very small difference in the observation between glass and quartz substrates. △ is used for the sample showing a dark colorful pattern.

The Raman spectra reported so far are for the films more than 25 μm thick. The oblique setting used here made it possible to measure the spectra of the thinner films. The Raman spectra for the MBBA thin (*ca.* 1 μm) film with a polarized incident light are shown in Fig. 2 ($\theta=60°$) for the 1700—1000 cm^{-1} region. (A) and (B) show the spectra for homogeneous (silk treatment) and homeotropic (0.7 mM HTAB treatment) samples respectively. For the homogeneous sample, the band intensities at 1598 cm^{-1} and 1577 cm^{-1} for $\boldsymbol{p}//\boldsymbol{E}$ are about three times larger than those for $\boldsymbol{p}\perp\boldsymbol{E}$, while for the homeotropic sample they are almost the same for $\boldsymbol{p}//\boldsymbol{E}$ and $\boldsymbol{p}\perp\boldsymbol{E}$, taking the electric vector of the incident light as $\boldsymbol{E}//\boldsymbol{a}$ and the long axis of the plate as $\boldsymbol{p}$. These spectra were independent of θ. The 1598 cm^{-1} and 1577 cm^{-1} bands are assigned to the benzene ring-vibrations,[3,4,12] the Raman-scattering tensors of which have the largest element $|\alpha'_{zz}|$ ($|\alpha'_{zz}|\gg|$other element$|$), taking z as the molecular long axis.

The Raman-scattering tensor (polarizability tensor derivative) is expressed by;

$$\alpha'_{\mathrm{mol}}=\begin{pmatrix}\alpha'_{xx} & \alpha'_{xy} & \alpha'_{xz}\\ \alpha'_{yx} & \alpha'_{yy} & \alpha'_{yz}\\ \alpha'_{zx} & \alpha'_{zy} & \alpha'_{zz}\end{pmatrix}, \tag{1}$$

where x, y, and z are the principal molecular axes. Assuming an axial symmetry about the z axis resulting from the free rotation around the z axis, we obtain $\alpha'_{zz}=\mathrm{A}$, $\alpha'_{zx}=\alpha'_{yz}=\alpha'_{zy}=\alpha'_{xz}=\mathrm{B}$, $\alpha'_{xx}=\alpha'_{yy}=\mathrm{C}$, and $\alpha'_{xy}=\alpha'_{yx}=\mathrm{D}$; then,

$$\alpha'_{\mathrm{mol}}=\begin{pmatrix}\mathrm{C} & \mathrm{D} & \mathrm{B}\\ \mathrm{D} & \mathrm{C} & \mathrm{B}\\ \mathrm{B} & \mathrm{B} & \mathrm{A}\end{pmatrix}. \tag{2}$$

The Raman-scattering tensor in the laboratory coordinates (space fixed, a, b, c);

$$\alpha'_{\mathrm{lab}}=\begin{pmatrix}\alpha'_{aa} & \alpha'_{ba} & \alpha'_{ac}\\ \alpha'_{ba} & \alpha'_{bb} & \alpha'_{bc}\\ \alpha'_{ac} & \alpha'_{bc} & \alpha'_{cc}\end{pmatrix} \tag{3}$$

is transformed from (1) or (2) using Euler's angles (α, β, γ).[19]

$$\begin{aligned}\alpha'_{aa}=&\,(1/3)(2C+A)+(1/3)(A-C)(3\sin^2\beta\cos^2\alpha-1)\\ &-D[\sin2\gamma(\cos^2\beta\cos^2\alpha-\sin^2\alpha)+\cos2\gamma\cos\beta\sin2\alpha]\\ &+B\sin\beta(2\cos\gamma\cos\beta\cos^2\alpha-\sin\gamma\sin2\alpha)\\ &-B\sin\beta(2\sin\gamma\cos\beta\cos^2\alpha+\cos\gamma\sin2\alpha).\end{aligned}$$

$$\begin{aligned}\alpha'_{ac}=&\,(A-C)\sin\beta\cos\beta\cos\alpha\\ &+D\sin\beta(\sin2\gamma\cos\beta\cos\alpha+\cos2\gamma\sin\alpha)\\ &+B(\cos\gamma\cos2\beta\cos\alpha-\sin\gamma\cos\beta\sin\alpha)\\ &-B(\sin\gamma\cos2\beta\cos\alpha+\cos\gamma\cos\beta\sin\alpha).\end{aligned}$$

$$\begin{aligned}\alpha'_{bc}=&\,(A-C)\sin\beta\cos\beta\sin\alpha\\ &+D\sin\beta(\sin2\gamma\cos\beta\sin\alpha-\cos2\gamma\cos\alpha)\\ &+B(\cos\gamma\cos2\beta\sin\alpha+\sin\gamma\cos\beta\cos\alpha)\\ &-B(\sin\gamma\cos2\beta\sin\alpha-\cos\gamma\cos\beta\cos\alpha).\end{aligned}$$

$$\begin{aligned}\alpha'_{ba}=&\,(1/2)(A-C)\sin^2\beta\sin2\alpha\\ &-(D/2)[\sin2\gamma(1+\cos^2\beta)\sin2\alpha-2\cos2\gamma\cos\beta\cos2\alpha]\\ &+B\sin\beta(\cos\gamma\cos\beta\sin2\alpha+\sin\gamma\cos2\alpha)\\ &-B\sin\beta(\sin\gamma\cos\beta\sin2\alpha-\cos\gamma\cos2\alpha).\end{aligned}$$

α'_{bb} and α'_{cc} are omitted.

In our Raman measurements, shown in Fig. 1, we observe $(\alpha'_{aa})^2+(\alpha'_{ac})^2$ as the intensities. Assuming the molecular long axis, z, to be parallel to $\boldsymbol{p}$ for the homogeneous samples and perpendicular to $\boldsymbol{p}$ for the homeotropic samples, Euler's angles for the sample settings are given as follows:

$\alpha=0°$, $\beta=90°$ for homogeneous $\boldsymbol{p}//\boldsymbol{E}$,

$\alpha=270°$, $\beta=30°$ for homogeneous $\boldsymbol{p}\perp\boldsymbol{E}$,

$\alpha=90°$, $\beta=60°$ for homeotropic $\boldsymbol{p}//\boldsymbol{E}$ and $\boldsymbol{p}\perp\boldsymbol{E}$.

The $(\alpha'_{aa})^2+(\alpha'_{ac})^2$ are calculated by averaging over $\gamma(0\rightarrow2\pi)$

$$
\begin{aligned}
(\alpha'_{aa})^2 + (\alpha'_{ac})^2 &= A^2 + B^2, \text{ for homogeneous } \boldsymbol{p}//\boldsymbol{E}\\
&= (3/4)B^2 + C^2 + (5/8)D^2,\\
&\qquad \text{for homogeneous } \boldsymbol{p}\perp\boldsymbol{E}\\
&= (1/4)B^2 + C^2 + (7/8)D^2,\\
&\qquad \text{for homeotropic } \boldsymbol{p}//\boldsymbol{E} \text{ and } \boldsymbol{p}\perp\boldsymbol{E}.
\end{aligned}
$$

Since we have $|A_1| \gg |B_1|$ and negligibly small $|C_1|$ and $|D_1|$ values for the 1598 cm^{-1} band (using the suffix 1), the larger intensity observed for the homogeneous $\boldsymbol{p}//\boldsymbol{E}$ than that for the homogeneous $\boldsymbol{p}\perp\boldsymbol{E}$ can well be interpreted. The intensity ratio between 1598 cm^{-1} and 1577 cm^{-1} bands should be constant for all the sample settings, which is in harmony with the observation. The observed Raman spectra, therefore, certainly confirm the molecular alignments suggested by the observation by a polarizing microscope; the molecular long axis is parallel to $\boldsymbol{p}$ for the homogeneous sample and perpendicular to $\boldsymbol{p}$ for the homeotropic sample.

The observed peak intensity ratios between the 1627 cm^{-1} and 1598 cm^{-1} bands are given in Table 2 for the MBBA thin films at $\theta=60°$, together with the value for the isotropic bulk (50 °C). If the 1627 cm^{-1} band is assigned to the C=N stretching vibration (using the suffix 2), $|B_2|$ and $|C_2|$ are quite large, though $|A_2|$ is the largest among $|A_2|$, $|B_2|$, $|C_2|$, $|D_2|$, because the C=N bond lies on the phenyl plane and makes an angle of 30° with the z axis.[12] The intensity ratio between the 1627 cm^{-1} and 1598 cm^{-1} bands, $I(1627)/I(1598)$, therefore, should vary with the molecular orientation, having the largest value for the homeotropic sample ($\boldsymbol{p}//\boldsymbol{E}$ and $\boldsymbol{p}\perp\boldsymbol{E}$). Based on the expressions for $(\alpha'_{aa})^2+(\alpha'_{ac})^2$ and the observed relation $|A_1|>|A_2|$, the following relation for the intensity ratio, $I(1627)/I(1598)$, can be derived:

$$
(\text{homogeneous } \boldsymbol{p}//\boldsymbol{E}) < (\text{homogeneous } \boldsymbol{p}\perp\boldsymbol{E}) < (\text{homeotropic } \boldsymbol{p}//\boldsymbol{E} \text{ and } \boldsymbol{p}\perp\boldsymbol{E}).
$$

Table 2. Intensity ratios between 1627 cm^{-1} and 1598 cm^{-1} bands, $I(1627)/I(1598)$, of MBBA films

	Bulk Isotropic	Film	
		Homogeneous	Homeotropic
$\boldsymbol{p}//\boldsymbol{E}$	0.417	0.402	0.445
$\boldsymbol{p}\perp\boldsymbol{E}$		0.414	0.445

The relation derived above is in good agreement with the observed values in Table 2. This fact also confirms that the 1627 cm^{-1} band is to be assigned to the C=N stretching vibration, though there may be some vibrational coupling with the benzene-ring vibration. The treatment described above is rather rough, and we have neglected the molecular precessional motion[5,12] around the optic axis.

The molecular orientation of the liquid crystals depends on the concentrations of HTAB or lecithin solutions as well as on the materials used for the pretreatment of the plates, as has been reported by Proust and Ter-Minassian-Saraga.[13] The Raman intensity ratios, $I(1627)/I(1598)$, observed for the samples treated with various concentrations of HTAB and lecithin are shown in Table 3. For the sample treated with 0.7 mM HTAB, the measurements were made for a number of samples, while for the other cases several samples were measured for each concentration. With the HTAB treatments the MBBA molecules were almost perpendicular to the plate surface, but with the lecithin treatments they were perpendicular only if a concentration of lecithin larger than 0.1 mM was used. Moreover, with 0.01 or 0.001 mM lecithin treatment the MBBA molecules were parallel to the plate surface. With low concentrations, the amount of the adsorbed HTAB or lecithin must be small, giving rise to an incomplete surface treatment.

Table 3. Relation between Raman intensity ratios of MBBA films and concentrations of HTAB and lecithin

Treatment		$I(1627)$/$I(1598)$	Microscopic observation
	Concentration		
HTAB (aq soln)	0.0070 mM	0.43_6	△
	0.070	0.44_1	⊥
	0.70	0.445	⊥
	1.4	0.44_5	⊥
Lecithin (C_2H_5OH soln)	0.0010 mM	0.39_7	∥
	0.010	0.40_1	∥
	0.10	0.43_2	⊥
	1.0	0.43_8	⊥

Table 4. Polarization components of 1598 cm^{-1} band of MBBA films (relative values)

	Homogeneous $\boldsymbol{p}//\boldsymbol{E}$	Homeotropic $\boldsymbol{p}//\boldsymbol{E}$, $\boldsymbol{p}\perp\boldsymbol{E}$
(aa)	1.0	1.0
(ac)	0.37	0.90
(bc)	0.29	1.6
(ba)	0.59	1.3

Thus, the intensity ratio provides a semi-quantitative measure of the molecular orientation. It was, however, found that the Raman results did not always coincide with those suggested by the polarizing microscopic observations. For example, the MBBA sample treated with 0.007 mM HTAB showed the Raman intensity ratio of 0.436, corresponding to the almost perpendicular orientation structure, though the examination by the polarizing microscope did not enable us to distinguish the molecular orientation.

The Raman intensity ratio varies with the change in the thickness of the samples. For the MBBA samples treated with 0.7 mM HTAB, the intensity ratio $I(1627)/I(1598)$ was 0.445 for the *ca.* 1 μm film and 0.427 for the 25—100 μm films ($\boldsymbol{p}//\boldsymbol{E}$, $\theta=60°$), showing that the molecular orientations were incomplete with the thicker films, because the ratio becomes largest when the molecules are perpendicular to the plate surface. On the other hand, the samples treated with silk did not show any appreciable change in the intensity ratio for 1—100 μm films.

The polarization components were measured for (aa), (ac), (bc), and (ba), where (ac) means the spectrum observed with a incident and c scattered components. The relative intensities of the 1598 cm^{-1} band observed among the polarization components

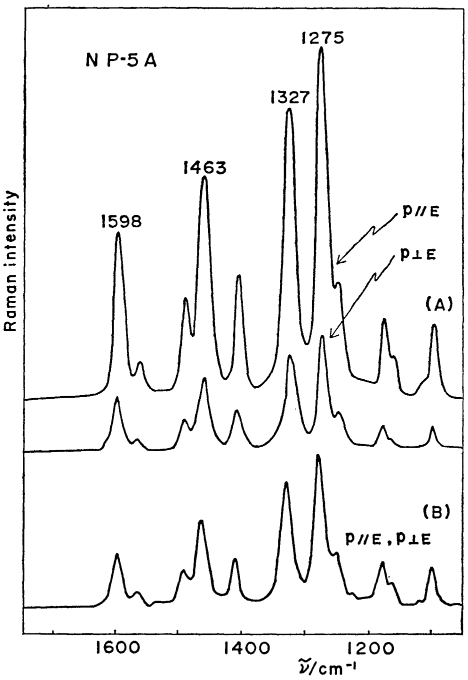

Fig. 3. Raman spectra of aligned thin (*ca.* 1 μm) films of NP-5A.
(A): Homogeneous, (B) homeotropic samples.

for $\theta=60°$ are shown in Table 4. The polarization components are calculated from the elements of α'_{1ab} derived above. For homogeneous $\boldsymbol{p}//\boldsymbol{E}$, $(\alpha'_{bc})^2=D_1^2/2$ and $(\alpha'_{ba})^2=B_1^2$ while for homeotropic $\boldsymbol{p}//\boldsymbol{E}$ and $\boldsymbol{p}\perp\boldsymbol{E}$,

$$(\alpha'_{bc})^2 = (3/16)A_1^2 + (1/4)B_1^2 + (3/16)C_1^2 + (3/32)D_1^2$$

$$(\alpha'_{ba})^2 = (3/4)B_1^2 + (1/8)D_1^2.$$

Then, for the 1598 cm^{-1} band, the following relations can be derived theoretically:

$(\alpha'_{bc})^2 < (\alpha'_{ba})^2$ for homogeneous $\boldsymbol{p}//\boldsymbol{E}$, and

$(\alpha'_{bc})^2 > (\alpha'_{ba})^2$ for homeotropic $\boldsymbol{p}//\boldsymbol{E}$ and $\boldsymbol{p}\perp\boldsymbol{E}$.

These relations are in harmony with the observed relations:

$I(\mathrm{bc}) < I(\mathrm{ba})$ for homogeneous $\boldsymbol{p}//\boldsymbol{E}$, and

$I(\mathrm{bc}) > I(\mathrm{ba})$ for homeotropic $\boldsymbol{p}//\boldsymbol{E}$ and $\boldsymbol{p}\perp\boldsymbol{E}$.

In this case, the values depend on θ. These results also confirm the molecular arrangements described above.

The results obtained for the NP-5A film samples are shown in Fig. 3 and Tables 5 and 6. For the NP-5A film, the Raman bands have not yet been assigned to the normal vibrations of the molecules. However, as is shown in Fig. 3 for the homogeneous sample treated with silk, the Raman intensities of the 1598, 1463, 1327, and 1275 cm^{-1} bands were much stronger for $\boldsymbol{p}//\boldsymbol{E}$ than those for $\boldsymbol{p}\perp\boldsymbol{E}$, while no appreciable intensity changes in these Raman bands could be observed for the homeotropic sample treated with 0.1 mM lecithin. The strong bands observed for the $\boldsymbol{p}//\boldsymbol{E}$ of the homogeneous sample can be assigned to the vibrations, of which the Raman-scattering tensors have the largest $|\alpha'_{zz}|$ values. This homogeneous sample showed a colorful texture in the polarizing microscopic examination and had its molecular axes parallel to $\boldsymbol{p}$. The sample treated with 0.7 mM HTAB also showed a colorful pattern, but not a colorful texture, and it was a kind of homogeneous sample where the molecular long axes must be randomly oriented on the plane parallel to the plate surface. In the homogeneous (texture) sample, the Raman intensity ratios are different for $\boldsymbol{p}//\boldsymbol{E}$ and $\boldsymbol{p}\perp\boldsymbol{E}$, while they are the same in the other cases, as is shown in Table 5.

TABLE 5. INTENSITY RATIOS FOR NP-5A FILMS

	Silk		0.7 mM HTAB	0.1 mM Lecithin
	$\boldsymbol{p}//\boldsymbol{E}$	$\boldsymbol{p}\perp\boldsymbol{E}$	$\boldsymbol{p}//\boldsymbol{E}$, $\boldsymbol{p}\perp\boldsymbol{E}$	$\boldsymbol{p}//\boldsymbol{E}$, $\boldsymbol{p}\perp\boldsymbol{E}$
$\dfrac{I(1278)}{I(1598)}$	2.4_4	2.1_6	2.1_8	2.3_5
$\dfrac{I(1327)}{I(1598)}$	1.9_0	1.8_3	1.8_6	2.0_5
$\dfrac{I(1463)}{I(1598)}$	1.3_9	1.3_9	1.4_5	1.4_9

TABLE 6. POLARIZATION COMPONENTS OF 1275 cm^{-1} BAND OF NP-5A FILMS (RELATIVE VALUES)

	Homogeneous (silk) $\boldsymbol{p}//\boldsymbol{E}$	Homeotropic (lecithin) $\boldsymbol{p}//\boldsymbol{E}$, $\boldsymbol{p}\perp\boldsymbol{E}$
(aa)	1.0	1.0
(ac)	0.6	0.8
(bc)	0.4	1.0
(ba)	0.6	0.7

The polarization components of the 1275 cm^{-1} band are shown in Table 6. $I(\mathrm{ba})>I(\mathrm{bc})$ was observed for the homogeneous sample and $I(\mathrm{bc})>I(\mathrm{ba})$ for the homeotropic sample, similar to those for the 1598 cm^{-1} band of MBBA films, confirming the molecular orientations suggested by the polarizing microscopic observations.

The infrared transmission spectra were observed at normal incidence for the MBBA films between quartz windows, but only in the C–H stretching region. They are shown in Fig. 4. The bands at 3022 and 3000 cm^{-1} can be assigned to the C–H stretching vibrations in =C–H or aromatic C–H groups. These bands have their transition moments on the molecular plane, because the C–H bands must be on the plane which approximately coincides with the benzene-ring planes. These bands are stronger for the homogeneous sample than for the homeotropic sample, as is shown in Fig. 4(A). The dichroic spectra for the homogeneous sample are observed to be as in Fig. 4(B), where these bands are stronger for $\boldsymbol{p}\perp\boldsymbol{E}$ than for $\boldsymbol{p}//\boldsymbol{E}$, taking the electric vector as $\boldsymbol{E}$. Bulkin and Lok, after measuring the far-infrared spectra of aligned films of MBBA, reported that the spectra of the homogeneous and homeotropic samples did not show any measurable difference in the intensity of the intermolecular mode.$^{9)}$ However, the present infrared results for the intramolecular modes can confirm the molecular orientations described above.

It may thus be considered that the Raman spectra certainly give information on molecular orientation

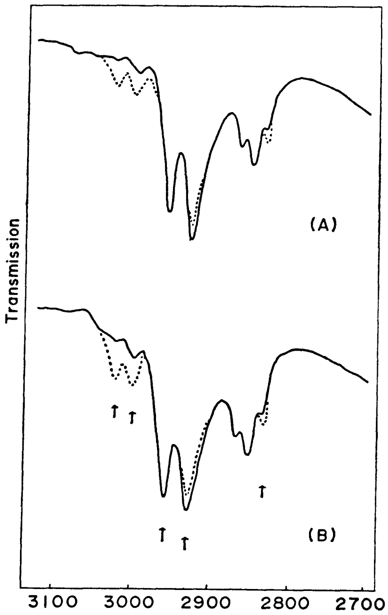

Fig. 4. Infrared spectra of aligned thin (*ca.* 1 μm) films of MBBA.
(A): Homeotropic —— and homogeneous ---- samples, (B): dichroism of homogeneous sample; ***p*//*E*** ——, ***p*⊥*E*** ----.

structures semiquantitatively. For the completely oriented structures, perpendicular or parallel, the Raman results agree well with the suggestions of the polarizing microscopic observations. Although the examination by a polarizing microscope is a simple and convenient method for distinguishing the orientations, it can not always be used, especially for the intermediate orientations. On the other hand, the Raman intensities measured can serve as a degree of alignment for the structural study of liquid crystal films. Furthermore, measurements of the thinner layers, more specific for the surface species, can be performed by observing the resonance Raman spectra, since the resonance Raman effect has been effectively used in the studies of small amounts of surface species.[14-17] Moreover, some theoretical work which assumes the molecular model parameters, such as the order parameter, developed by Pershan *et al.*[5] and Hatta,[12] will be able to quicken progress in studying the structures in their molecular dimensions.

Lastly, let us add some consideration of the mechanism of the formation of the two types of molecular orientation structures, homogeneous and homeotropic. The homogeneous structures appeared in thin films between two silk-treated clean plates, while the homeotropic structures appeared in thin films between plates previously treated with HTAB or lecithin solutions of certain concentration ranges. In the former case, it is supposed that the long molecules of liquid crystals with dipoles whose moment vectors being considered are in the direction of their long axes will be attracted to the plate surface mainly by the electrostatic forces between their dipoles and induced dipoles at the surface, and that they will also be oriented parallel to the surface in the inner part of the films by means of the dipole-dipole interactions, so that they will realize the homogeneous structures. On the other hand, in the latter case, where the plates are pretreated with HTAB or lecithin, whose molecules are amphiphilic in nature, the plate surfaces will be covered by these molecules anchored by their polar groups and will, accordingly, become hydrophobic because of the hydrocarbon chains oriented outside. Then, the liquid-crystal molecules with also hydrophobic groups (hydrocarbon chains at the end of their long molecules) will be attracted to the hydrophobic surfaces by the London-van der Waals attraction forces,[18] so that they will be oriented perpendicular to the surface to form homeotropic structures. However, if the concentration of the HTAB or lecithin solution used for pretreatment is too low, the surface density of the adsorbed molecules will be too small to realize the favorable orientation of the homeotropic alignment of the liquid-crystal molecules. Moreover, the difference observed between HTAB and lecithin in the concentration ranges (0.01 mM<for HTAB, 0.1 mM< for lecithin) required for the homeotropic alignment may be considered to be due to the difference in their molecular structures regarding the possibility of taking favorable orientations at the solid surface.

We wish to acknowledge the financial support from the Mitsubishi Foundation.

References

1) L. Verbit, *J. Chem. Educ.*, **49**, 36 (1972).
2) T. Uchida, H. Watanabe, and M. Wada, *Jpn. J. Appl. Phys.*, **11**, 1559 (1972).
3) G. Vergoten and G. Fleury, *Mol. Cryst. Liq. Cryst.*, **30**, 213 (1975); **36**, 327 (1976).
4) G. Vergoten and G. Fleury, *J. Mol. Struct.*, **30**, 347 (1976).
5) S. Jen, N. A. Clark, P. S. Pershan, and E. B. Priestley, *J. Chem. Phys.*, **66**, 4635 (1977); *Phys. Rev. Lett.*, **31**, 1552 (1973).
6) J. Le Brumant, N. A. Tuan, and M. Jaffrain, *C. R. Acad. Sci., Ser. B*, **280**, 719 (1975).
7) F. Cavatorta, M. P. Fontana, and N. Kirov, *Mol. Cryst. Liq. Cryst.*, **34**, 241 (1977).
8) H. Yamada, Y. Yamamoto, K. Fukumura, and B. Tamamushi, *Chem. Lett.*, **1978**, 345.
9) B. J. Bulkin and W. B. Lok, *J. Phys. Chem.*, **77**, 320 (1973).
10) M. Evans, M. Davies, and L. Larkin, *J. Chem. Soc., Faraday Trans. 2*, **69**, 1011 (1973).
11) E. Sciesinska, J. Sciesinski, J. Twardowski, and J. A. Janik, *Mol. Cryst. Liq. Cryst.*, **27**, 125 (1974).
12) A. Hatta, *Bull. Chem. Soc. Jpn.*, **50**, 2522 (1977); A. Hatta, H. Nohara, and W. Suëtaka, *ibid.*, **51**, 967 (1978).
13) J. E. Proust and L. Ter-Minassian-Saraga, *J. Phys. (Paris)*, **36**, Cl-77 (1975).
14) T. Nagasao and H. Yamada, *J. Raman Spectrosc.*, **3**, 153 (1975).
15) Y. Yamamoto and H. Yamada, *J. Chem. Soc., Faraday Trans. 1*, **74**, 1562 (1978); H. Yamada and Y. Yamamoto, *ibid.*, **75**, 1215 (1979).
16) H. Yamada, T. Amamiya, and H. Tsubomura, *Chem. Phys. Lett.*, **56**, 591 (1978).
17) H. Yamada, *Indian J. Pure Appl. Phys.*, **16**, 159 (1978).
18) F. London, *Z. Phys.*, **63**, 245 (1930).
19) M. E. Rose, "Elementary Theory of Angular Momentum," Wiley, New York (1957), p. 50.
20) K. Fukumura, Master's thesis, Kwansei Gakuin University (1980).